COMMUNICATION

Incarceration of iodine in a pyrene-based metal–organic framework

Andrzej Gładysiak,†[a] Tu N. Nguyen,†[a] Mariana Spodaryk,[b] Jung-Hoon Lee,[c,d] Jeffrey B. Neaton,[c,d,e] Andreas Züttel,[b] and Kyriakos C. Stylianou*[a]

Abstract: A pyrene-based metal–organic framework (MOF) **SION-8** captures iodine (I_2) vapour with a capacity of 460 mg g^{-1}_{MOF} and 250 mg g^{-1}_{MOF} at room temperature and at 75 °C, respectively. Single-crystal X-ray diffraction analysis and van der Waals-corrected density functional theory calculations confirm the presence of I_2 molecules within the pores of **SION-8** and their interaction with the pyrene-based ligands. The I_2-pyrene interactions in the I_2-loaded **SION-8** lead to a 10^4-fold increase of its electrical conductivity compared to the bare **SION-8**. Upon adsorption, ≥95% of I_2 molecules are incarcerated and cannot be washed out, signifying the potential of **SION-8** towards the permanent capture of radioactive I_2 at room temperature.

Radioactive isotopes of iodine, mainly ^{129}I and ^{131}I, are produced in nuclear-related processes and may accidentally be released into the atmosphere as witnessed in Fukushima and Chernobyl, constituting a major hazard to humans and the environment. The ^{131}I has a radioactive decay half-life of ~8 days, emits β^- and γ rays, and concentrates in the thyroid gland of the person exposed to the radioactive source causing thyroid cancer. The ^{129}I isotope is much longer lived, with a half-life of 15.7 million years, and poses a long-term disposal risk. Capturing radioactive iodine is therefore necessary for safe nuclear waste storage.[1]

Wet scrubbing and the use of solid adsorbents are two general methods for iodine capture, with the latter being often preferred since it does not require the use of highly corrosive liquids.[1] The benchmark solid adsorbents for radioactive iodine capture is the silver (Ag)-exchanged zeolitic mordenite, with an average I_2 adsorption capacity of ~100–130 mg $g^{-1}_{mordernite}$ at high temperatures (150–200 °C).[1-2] In recent years, metal–organic frameworks (MOFs), which are crystalline materials formed by linking metal ions or metal clusters with multi-topic organic ligands,[3] have emerged as promising adsorbents for I_2 capture due to their high porosity[4] and chemical tuneablility.[5] For example, our group has previously reported a high I_2 vapour uptake by HKUST-1 and ZIF-8, and their composites with polymers, reaching 538 mg $g^{-1}_{HKUST-1}$ at 75 °C.[6] The Nenoff group and the Thallapally group have studied the adsorption of I_2 on HKUST-1 and SBMOFs, respectively, in the presence of humidity.[7] However, the degradation of these MOFs in water, and the leaching of I_2 from the I_2-loaded MOFs when they are in contact with water and common organic solvents give rise to considerable concerns regarding the potential of these MOFs for I_2 capture. The I_2 leaching is thought to be due to the weak interaction between the I_2 molecules with the pore surface of the MOF.

Herein, we report a MOF named **SION-8**, which is based on the employment of 1,3,6,8-tetrakis(*p*-benzoic acid)pyrene (H_4TBAPy) and Ca^{II},[8] that can efficiently capture I_2 vapour at both room temperature and at 75 °C. The strategy for I_2 capture is based on the well-known donor–acceptor interaction between pyrene and I_2.[9] We will present single-crystal X-ray diffraction (SCXRD), impedance spectroscopy, and gravimetric studies as well as van der Waals-corrected density functional theory (vdW-corrected DFT) calculations to elucidate the location and interaction between I_2 and the pyrene-decorated pore surface of **SION-8**.

SION-8 was synthesized from the self-assembly of Ca^{II} ions with the $TBAPy^{4-}$ ligand in an acidified mixture of DMF and water, giving rise to single crystals of $[Ca_2(TBAPy)(\mu_2\text{-}OH_2)_2]\cdot 2DMF$. **SION-8** crystallizes in the orthorhombic space group *Pbam*, and its structure is based on 1-dimensional Ca–O chains extending along the *a*-axis interlinked by the fully deprotonated $TBAPy^{4-}$. Structural analysis reveals two symmetrically inequivalent channels across the structure of **SION-8**, one of which is exposed to the lateral sides of the $TBAPy^{4-}$ ligands and hence possesses a hydrophobic character, whilst the other one is surrounded by the O-atoms of the Ca–O chains and coordinated H_2O molecules which endow it with a more hydrophilic character. The combination of both the hydrophilic and hydrophobic pores accounts for an accessible volume of 24.8% of the unit cell.[8]

The phase purity of **SION-8** was confirmed by powder X-ray diffraction (PXRD). The experimental PXRD pattern of **SION-8** can be indexed with the cell parameters of its crystal structure (Figure S1). The framework is stable in aqueous solution for at least 24 hours as confirmed by PXRD (Figure S2). The thermogravimetric profile of **SION-8** (Figure S3) displays multiple steps due to the stepwise removal of the DMF molecules in the

[a] A. Gładysiak, Dr. T. N. Nguyen, Dr. K. C. Stylianou
Laboratory of Molecular Simulation (LSMO),
Institut des sciences et ingénierie chimiques (ISIC),
École polytechnique fédérale de Lausanne (EPFL Valais),
Rue de l'Industrie 17, 1951 Sion (Switzerland)
E-mail: kyriakos.stylianou@epfl.ch
[b] Dr. M. Spodaryk, Prof. Dr. A. Züttel
Laboratory of Materials for Renewable Energy (LMER),
Institut des sciences et ingénierie chimiques (ISIC),
École polytechnique fédérale de Lausanne (EPFL Valais),
Rue de l'Industrie 17, 1951 Sion (Switzerland)
[c] Dr. J.-H. Lee, Prof. Dr. J. B. Neaton
Molecular Foundry, Lawrence Berkeley National Laboratory,
Berkeley, California 94720 (USA)
[d] Dr. J.-H. Lee, Prof. Dr. J. B. Neaton
Department of Physics, University of California,
Berkeley, California 94720 (USA)
[e] Prof. Dr. J. B. Neaton
Kavli Energy Nanosciences Institute at Berkeley,
Berkeley, California 94720 (USA)
† The authors contributed equally.

Supporting information for this article is given via a link at the end of the document.

hydrophobic and hydrophilic pores and the release of the coordinated H_2O molecules. As a consequence, **SION-8** can be partially activated by removing the DMF molecules present in the hydrophobic pores, or fully activated by completely removing all the lattice solvents. However, this is only at the partially activated state that the crystal singularity of **SION-8** is retained. The Brunauer–Emmett–Teller (BET) surface areas for the partially and fully activated **SION-8** samples are 174 $m^2\ g^{-1}$ and 509 $m^2\ g^{-1}$, respectively (Figure S4).[8]

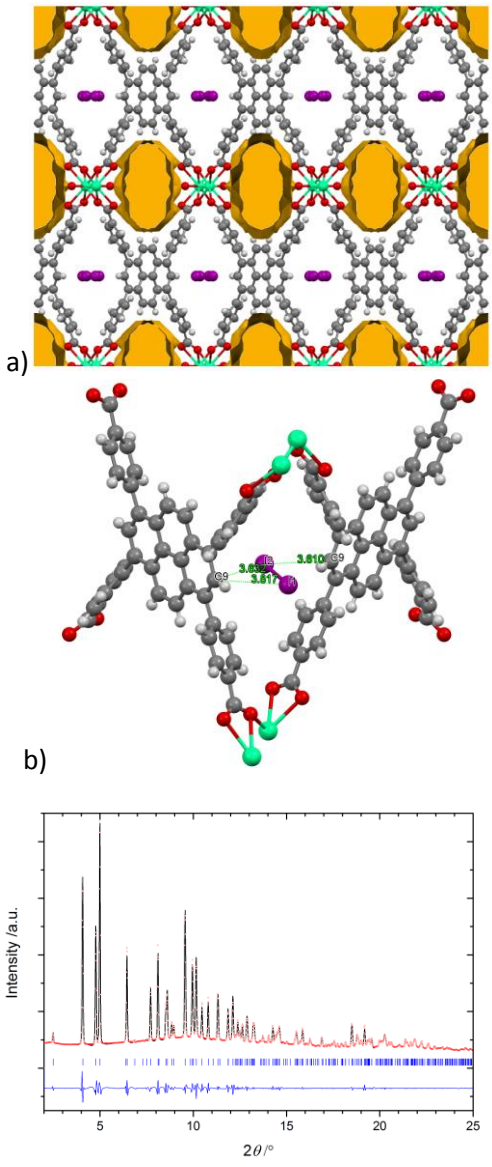

Figure 1. (a) Crystal structure of **SION-8⊃I_2** viewed along the *a*-axis. Atom color code: green, Ca; purple, I; red, O; grey, C; white, H. Disordered solvent-containing structural voids have been depicted as gold surfaces. (b) Localization of the I_2 molecule within the hydrophobic pore of **SION-8**. Precise values of the highlighted closest I_2–$TBAPy^{4-}$ distances are: I2–C9 = 3.609(15) Å, I2–C9' = 3.64(2) Å, I1–C9' = 3.817(18) Å. (c) PXRD Le Bail refinement of **SION-8⊃I_2** (space group *Pbam*: R_p = 2.09%, R_{wp} = 2.78%; *a* = 6.8361(2) Å, *b* = 20.3071(7) Å, *c* = 16.5648(6) Å, λ = 0.72179 Å). Experimental data are shown as black plots, the refined Le Bail profiles as red dots, and the difference between them as blue plots. Reflection positions are marked with blue.

When the partially activated single crystals of **SION-8** were exposed to I_2 vapour at room temperature, the yellow colour of the crystals slowly turned to black purple. After 72 h of I_2 loading, a single crystal was picked to investigate its structure with SCXRD (Table S1). **SION-8⊃I_2** conserves the original framework connectivity of **SION-8** (Figure 1a). I_2 molecules were found to be located within the pores of the framework, with an average of 0.405 I_2 molecules in each hydrophobic pore; simultaneously, the hydrophilic pores are occupied by the disordered DMF solvent molecules. The formula of this material sums up to $[Ca_2(TBAPy)(H_2O)_2]\cdot DMF\cdot 0.81I_2$. Both atoms of the I_2 molecule, named I1 and I2, are located at special positions with the crystallographic occupancy of 0.5, while their site occupancy factor refines to 0.405(9). The I1–I2 distance equals 2.73(2) Å, which is comparable to the I–I separations reported in other crystal structures (Figure S5) and our DFT-computed value (2.688 Å). The I_2 molecule is nearly perpendicular to one pyrene core of $TBAPy^{4-}$ and nearly parallel to the neighbouring one with the shortest I_2–$TBAPy^{4-}$ distance of 3.609(15) Å (Figure 1b). Visualization of the crystal structure of **SION-8⊃I_2** may suggest the existence of infinite $(–I–I–)_n$ chains; however, since the I1 and I2 atom sites are not fully occupied, such chains are probably not formed.

The shapes of anisotropic displacement ellipsoids of I1 and I2 seem intricate; however, they conform to the 'rigid-bond postulate'.[10] The difference in the radii of the vibration ellipsoids of atoms I1 and I2 along the bond between them of 0.00021 $Å^2$ is situated below the limit imposed by the Hirshfeld test (0.001 $Å^2$).[11] Substantial improvement of refinement indicators when an I_2 molecule is introduced into the crystal structure (Table S2) makes still another argument in favour of the occurrence of I_2 molecules in the hydrophobic pores of **SION-8**. Further improvement of *R*-factors on squeezing[12] indicates the presence of heavily disordered DMF molecules in the hydrophilic pores. However, the results of squeezing of the 'bare' and the I_2-containing structure are virtually the same.

Inspired by the results of the crystallographic analysis, we investigated the time-dependent adsorption of I_2 vapour in the partially activated powder samples of **SION-8** at room temperature and at 75 °C. The I_2 adsorption can be visually observed as the yellow powder of **SION-8** quickly turns its colour to black purple. The PXRD pattern of the I_2-loaded sample is comparable with the one of **SION-8** (Figure 1c), with the Bragg reflections remaining at the same position although the intensity of several of them is lower (Figure S6). The decrease of the PXRD peaks' intensity is probably due to the I_2 molecules being incommensurate with the periodicity of the framework, and is also often observed in other guest@MOF systems.[13] As shown in Figure 2, at room temperature, I_2 is relatively quickly adsorbed and the uptake capacity reaches 34 wt% (340 mg g^{-1}_{MOF}) after 200 hours. The adsorption rate is then decreased, and by 1000 hours, the total adsorption is 46 wt% (460 mg g^{-1}_{MOF}). This corresponds to 1.6 I_2 molecules per formula unit of **SION-8**, which is matched by the result of the elemental analysis (Table S3). Since adsorption is an exothermic process, the equilibrium I_2 loading at 75 °C is shifted towards the substrates (compared with the case of room temperature) with the total adsorption of 25 wt% (250 mg g^{-1}_{MOF}). On the other hand, at 75 °C, the adsorption reaches saturation in a much shorter time, already after 2.5 h. Interestingly, when fully activated **SION-8** is used instead of the partially activated material, virtually the same adsorption figure was obtained, suggesting a preference of non-polar I_2 molecules to occupy solely the hydrophobic pores (Figure S7). The rate of adsorption at 75 °C is ~~in fact~~ five times greater than that of HKUST-1 crystalline powder, as 1 gram of

HKUST-1 adsorbs ~100 mg I_2 after 5 hours.[6] This also suggests that **SION-8** has high affinity towards I_2, most probably due to the strong interaction between the I_2 molecules and pyrene-decorated pore surface of **SION-8**. Based on our vdW-corrected DFT calculations which previously were shown to reliably quantify the host–guest interactions in MOF-based systems,[14] the computed I_2 binding energy is –73.2 kJ mol^{-1} which is comparable to those found in other charge transfer MOF–I_2 complexes (MOFs with open metal sites).[15] More interestingly, washing the **SION-8⊃I₂** powder with water or copious amounts of common organic solvents such as ethanol, toluene, and hexane gives rise to the release of only 5.0% of the captured I_2 (Figure S8).

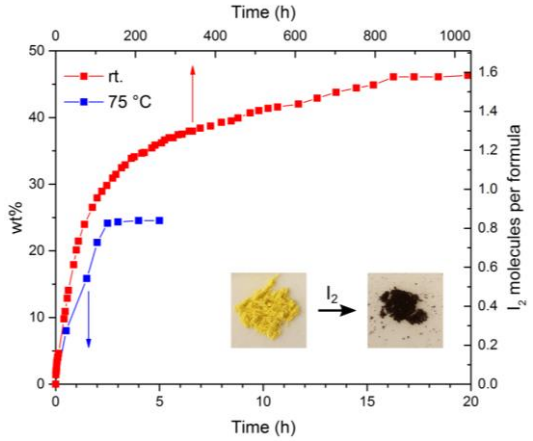

Figure 2. I_2 adsorption on partially activated **SION-8** at room temperature (red plots) and at 75 °C (blue plots). Note two different time scales for these processes. The inset comprises the photographs of **SION-8** and **SION-8⊃I₂** powder samples.

Thermal stability of **SION-8⊃I₂** was investigated with differential scanning calorimetry (DSC). Upon continuous heating, DSC profile of **SION-8⊃I₂** featured a broad endothermic peak starting at 70 °C and centred at 140 °C (Figure S9). This peak, however, was absent when the sample was cooled down to room temperature and heated up again during the second thermal cycle. Therefore, we associate that peak to the endothermic desorption of I_2 from within the pores of **SION-8⊃I₂**. This result signifies that I_2 can be permanently captured by partially activated **SION-8** in a broad range of temperatures spanning from room temperature up to ca. 70 °C. ZrDMBD-I_2 exhibited a similar thermal stability (up to 90 °C), however, in that case I_2 could be released by washing the sample with 1,2-ethanedithiol.[5a]

To investigate this interaction further, we first collected the diffuse reflectance spectra of **SION-8** and **SION-8⊃I₂** (Figure S10). **SION-8** displays a broad and strong absorption in the 250–500 nm region, with the peak centred at ~400 nm, which can be attributed to the π-π* transitions of the TBAPy^{4-} ligand. On the other hand, **SION-8⊃I₂** absorbs light in a very broad range of the visible region with the low-energy photon absorption threshold extending far into the IR region, suggesting the occurrence of a charge transfer process that significantly lowers the bandgap energy of the material. Similar phenomenon was observed for other I_2@MOFs; for example, Hu *et al.* reported the MOF $[Tb(Cu_4I_4)(ina)_3(DMF)]$ in which the I_2@$[Tb(Cu_4I_4)(ina)_3(DMF)]$ displayed a broad absorption over the visible window and its bandgap is 1.5 eV lower than the one of the bare MOF.[16] It is worth noting that the interaction of I_2 with aromatic compounds has been studied since the 1940s and the hypothesis was that I_2 has an abnormally high dielectric polarization in these liquids and forms complexes of solvent-I^+I^-.[17] In the case of pyrene (and other highly aromatic compounds), the donor–acceptor charge transfer between the pyrene molecule and I_2 leads to a high electrical conductivity of the pyrene–I_2 complex compared to its individual components.[9] Inspired by this study, we then performed the electrochemical impedance spectroscopy measurements on **SION-8** and **SION-8⊃I₂.** The powders of the samples (Table S4) were pressed into pellets and placed in a home-designed conductivity cell (Figure S11). The impedance spectra were obtained in the range of temperatures of 5–23 °C (Figures S12-S14). As can be observed in Figure 3, **SION-8⊃I₂** displays electrical conductivity that increases with increasing temperature and reaches σ = 5.3 × 10^{-6} S cm^{-1} at 23 °C. This value is comparable to those reported for other I_2@MOFs,[16, 18] although the latter were obtained from a variety of different methods;[19] similar in size increase of electrical conductivity was also reported for other MOF charge transfer complexes, namely by utilizing fullerenes and TCNQ as electron acceptors.[20] In contrast to the semiconducting behaviour of the I_2-captured sample, **SION-8** is an insulator (σ < 10^{-9} S cm^{-1}) and the semi-circular impedance spectrum for this material could not be obtained.

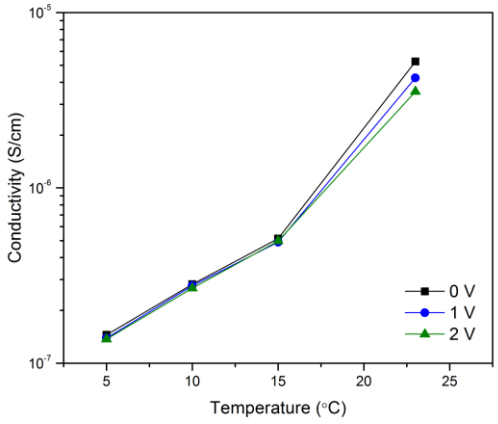

Figure 3. Electrical conductivity as a function of temperature collected on **SION-8⊃I₂**.

To further confirm the charge transfer interaction between the framework of **SION-8** and I_2, DFT calculations were performed. Figure S15 shows the optimized crystal structures of **SION-8** in the absence and presence of I_2 within its pores. In the structural optimizations, we fixed the experimental lattice parameters for both structures. For the **SION-8⊃I₂**, we considered an I_2 channel in the unit cell as shown in Figure S15b. Figure 4 shows the computed total and partial density of states (DOS) of the two structures. Since the contribution of Ca s and p orbitals to the projected DOS is negligible within the energy window shown in Figure 4, this contribution was excluded. As shown in Figure 4a, the valence band maximum (VBM) and conduction band minimum (CBM) levels of **SION-8** are mainly composed of C 2p character (Figure S16), and the calculated DFT-vdW-DF-cx band gap is 2.08 eV. For **SION-8⊃I₂**, interestingly, the CBM states are characterized by the I p character. As illustrated in Figure 4b, the I 5p–I 5p antibonding states are located above the VBM level and these states can be

clearly observed in the charge density at the CBM level (Figure S17). Due to this, the band gap is significantly reduced to 0.48 eV. Although DFT is known to underestimate the band gap,[21] it can often predict the trends in band gap.[22] Given the extended nature of both the C p and I p states along the pore direction (Figures S16 and S17), we expect the trend in the DFT-vdW-DF-cx band gap to be consistent with experiment in this case as well. This smaller band gap has in turn impact on the increase of the conductivity of **SION-8⊃I₂** compared to **SION-8**.

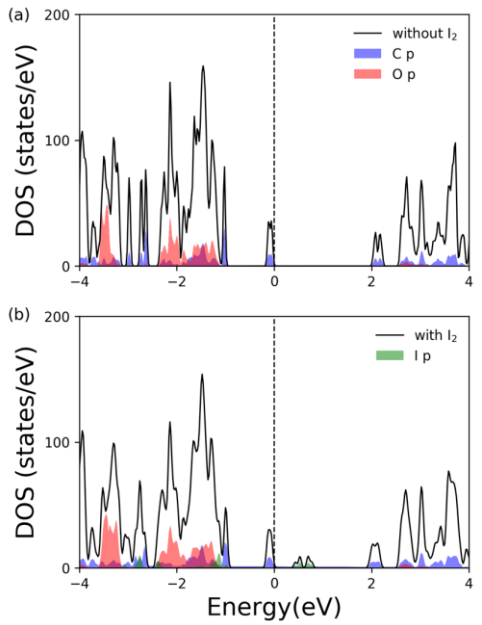

Figure 4. Computed total density of states (DOS, depicted as the black contour) and partial charge density (PDOS, coloured as a function of contributing element) of C, O and I atoms of (a) **SION-8** (b) **SION-8⊃I₂**

In summary, we report a pyrene-based MOF that can adsorb I_2 vapour with high capacity. The strong interaction between I_2 and the pyrene-based ligand of **SION-8** is due to the donor–acceptor charge transfer between them, and manifested by the changes in the photophysical and electrical properties of the MOF. This leads to the incarceration of I_2 within the MOF's cavity, suggesting the potential of **SION-8** for capturing radioactive I_2.

Experimental Section

Synthesis of SION-8 and iodine loading

The reaction between 10 mg (0.0680 mmol) of $CaCl_2{\cdot}2H_2O$ and 10 mg (0.0146 mmol) of H_4TBAPy (prepared using a previously reported procedure)[23] in the solution composed of 2 mL of *N,N*-dimethylformamide (DMF), 1 mL of H_2O and 80 µL of HCl (techn., 32%) at 120 °C for 72 h resulted in 11.85 mg (0.0126 mmol, 86.0% yield) of $[Ca_2(TBAPy)(\mu_2\text{-}OH_2)_2]{\cdot}2DMF$ (**SION-8**) in the form of single crystals.[8]

The crystals of **SION-8** were introduced into an open vial, which in turn was enclosed in a glass vessel containing solid iodine. The vial containing **SION-8** was repeatedly weighted to determine the increase of the mass of the sample. The procedure was repeated *i.* at room temperature and *ii.* at 75 °C.

Single-crystal X-ray diffraction analysis

A high-quality single crystal of **SION-8⊃I₂** was mounted onto a PILATUS@SNBL diffractometer at the BM01 beamline (European Synchrotron Radiation Facility, Grenoble, France),[24] and probed with X-rays (λ = 0.72179 Å). Preliminary exposures confirmed the singularity of the crystal. Reflection intensities were measured using the PILATUS2M detector. The crystal was kept at 100(2) K during data collection. Raw data were processed with CrysAlisPro (v. 1.171.38.43) program suite,[25] and the empirical absorption correction was performed using spherical harmonics, implemented in SCALE3 ABSPACK scaling algorithm. Crystal structure was solved with the SHELXT structure solution program using Intrinsic Phasing,[26] and refined with the SHELXL refinement package using least-squares minimization,[27] implemented in the Olex2 program suite.[28] Contribution of the disordered solvent molecules found in the structural voids to the measured structure factors was quantified with the SQUEEZE procedure of the PLATON program suite.[12] Solvent accessible volume of 571 Å^3 (24.8%) (probe radius 1.2 Å) was calculated with the program MERCURY (v. 3.10.1).[29] The difference in the radii of the vibration ellipsoids of atoms I1 and I2 along the bond between them of 0.00021 Å^2 was calculated with the program PLATON (v. 120716).[30]

Unit-cell parameters derived from the SCXRD study were used as a starting point of the full profile decomposition of the powder XRD pattern of **SION-8⊃I₂**. Fitting was performed using the FullProf program suite.[31] Le Bail-refined unit-cell parameters were a = 6.8361(2) Å, b = 20.3071(7) Å, c = 16.5648(6) Å, space group *Pbam*, λ = 0.72179 Å.

Impedance spectroscopy measurements

Conductivity of **SION-8⊃I₂** was investigated using electrochemical impedance spectroscopy (EIS). The measurements were performed on potentiostat/galvanostat PGSTAT302N with FRA32M module (Metrohm Autolab). Impedance spectra of the powder samples pressed into 8 mm diameter (thickness of 0.6–0.65 mm) pellets were measured in the range of working frequencies from 1 Hz to 1 MHz. The measurement frequency range is built using a logarithmic distribution. The voltage modulation amplitude was set to 10 mV. Pressed powder samples were investigated in home-designed conductivity cell with copper contacts previously plated with gold in order to assure their chemical stability during measurements. In order to achieve a sufficient contact between powder particles the measurements were carried out under the pressure of 1990 kG cm^{-2}. The impedance spectra were obtained in the range of temperatures of 5–23 °C.

Computational details

We perform first-principles density functional theory (DFT) calculations using the GBRV high-throughput ultrasoft pseudopotentials with the Quantum ESPRESSO plane wave DFT code.[33] To include the effect of the van der Waals (vdW) dispersive interactions, we perform structural relaxations with vdW dispersion-corrected functional (vdW-DF-cx)[34] as implemented in Quantum ESPRESSO. The initial structure is obtained from the experiment. For the structural relaxations, we fix the experimental lattice parameters and use a 3 × 1 × 1 Monkhorst−Pack *k*-point mesh centred at Γ and a 130 Ry plane-wave cutoff energy. For the density of states, we use a 6 × 2 × 2 Monkhorst−Pack *k*-point mesh centred at Γ. We explicitly treat seven valence electrons for I ($5s^2 5p^5$), ten for Ca ($3s^2 3p^6 4s^2$), six for O ($2s^2 2p^4$), four for C ($2s^2 2p^2$), and one for H($1s^1$). All structural relaxations are performed with a Gaussian smearing of 0.002 Ry.[35] The ions are relaxed until both the forces and energy are less than 0.5^{-3} Ry Bohr^{-1} and 0.5^{-4} Ry respectively.

To compute I_2 binding energies, we optimize **SION-8** prior to I_2 adsorption ($E_{\text{SION-8}}$), interacting with I_2 in the gas phase (E_{I2}) within a 15 Å × 15 Å × 15 Å cubic supercell, and **SION-8** with adsorbed I_2 molecules ($E_{\text{SION-8⊃I2}}$) using vdW-corrected DFT. The binding energies (E_B) are obtained via the difference:

$E_B = E_{SION\text{-}8\supset I2} - (E_{SION\text{-}8} + E_{I2})$.

Acknowledgements

KCS and TNN thank Swiss National Science Foundation (SNSF) for funding under the Ambizione Energy Grant no. PZENP2 166888 and NCCR: MARVEL – DD4.5. Access to the BM01 Swiss-Norwegian Beamline at the ESRF, Grenoble, France is gratefully acknowledged. AG and KCS thank Dr. Dmitry Chernyshov and Ms. Samantha L. Anderson for valuable discussions. JHL and JBN were supported by the Center for Gas Separations Relevant to Clean Energy Technologies, an Energy Frontier Research Center, funded by the U.S. Department of Energy, Office of Science, Office of Basic Energy Sciences, under Award DE-SC0001015. Work at the Molecular Foundry was supported by the Office of Science, Office of Basic Energy Sciences, U.S. Department of Energy, under Contract DE-AC02-05CH11231, and computational resources were provided by DOE (LBNL Lawrencium and NERSC).

Keywords: metal–organic framework • iodine capture • charge transfer • conductivity• impedance spectroscopy

[1] B. J. Riley, J. D. Vienna, D. M. Strachan, J. S. McCloy, J. L. Jerden, *J. Nucl. Mater.* **2016**, *470*, 307-326.

[2] (a) T. R. Thomas, B. A. Staples, L. P. Murphy, *Development of Ag^0Z for bulk ^{129}I removal from nuclear fuel reprocessing plants and PbX for ^{129}I storage*, **1978**; (b) R. T. Jubin, *Organic iodine removal from simulated dissolver off-gas systems utilizing silver-exchanged mordenite*, **1981**.

[3] (a) O. K. Farha, J. T. Hupp, *Acc. Chem. Res.* **2010**, *43*, 1166-1175; (b) H. Furukawa, K. E. Cordova, M. O'Keeffe, O. M. Yaghi, *Science* **2013**, *341*, 1230444; (c) M. L. Foo, R. Matsuda, S. Kitagawa, *Chem. Mater.* **2014**, *26*, 310-322.

[4] X. Zhang, I. da Silva, H. G. W. Godfrey, S. K. Callear, S. A. Sapchenko, Y. Cheng, I. Vitórica-Yrezábal, M. D. Frogley, G. Cinque, C. C. Tang, C. Giacobbe, C. Dejoie, S. Rudić, A. J. Ramirez-Cuesta, M. A. Denecke, S. Yang, M. Schröder, *J. Am. Chem. Soc.* **2017**, *139*, 16289-16296.

[5] (a) K. K. Yee, Y. L. Wong, Z. Xu, *Dalton Trans.* **2016**, *45*, 5334-5338; (b) A. S. Munn, F. Millange, M. Frigoli, N. Guillou, C. Falaise, V. Stevenson, C. Volkringer, T. Loiseau, G. Cibin, R. I. Walton, *CrystEngComm* **2016**, *18*, 8108-8114.

[6] B. Valizadeh, T. N. Nguyen, B. Smit, K. C. Stylianou, *Adv. Funct. Mater.* **2018**, *28*, 1801596.

[7] (a) D. F. Sava, K. W. Chapman, M. A. Rodriguez, J. A. Greathouse, P. S. Crozier, H. Zhao, P. J. Chupas, T. M. Nenoff, *Chem. Mater.* **2013**, *25*, 2591-2596; (b) D. Banerjee, X. Chen, S. S. Lobanov, A. M. Plonka, X. Chan, J. A. Daly, T. Kim, P. K. Thallapally, J. B. Parise, *ACS Appl. Mater. Interfaces* **2018**, *10*, 10622-10626.

[8] A. Gładysiak, K. S. Deeg, I. Dovgaliuk, A. Chidambaram, K. Ordiz, P. G. Boyd, S. M. Moosavi, D. Ongari, J. A. R. Navarro, B. Smit, K. C. Stylianou, *ACS Appl. Mater. Interfaces* **2018**, *10*, 36144–36156.

[9] M. Kawabe, K. Masuda, J. Yamaguchi, *J. Phys. Soc. Jpn.* **1968**, *24*, 1281-1285.

[10] M. Harel, F. L. Hirshfeld, *Acta Cryst. Sect. B* **1975**, *31*, 162-172.

[11] F. Hirshfeld, *Acta Cryst. Sect. A* **1976**, *32*, 239-244.

[12] A. Spek, *Acta Cryst. Sect. C* **2015**, *71*, 9-18.

[13] (a) R. X. Yao, X. Cui, X. X. Jia, F. Q. Zhang, X. M. Zhang, *Inorg. Chem.* **2016**, *55*, 9270-9275; (b) S. S. Lobanov, J. A. Daly, A. F. Goncharov, X. Chan, S. K. Ghose, H. Zhong, L. Ehm, T. Kim, J. B. Parise, *J. Phys. Chem. A* **2018**, *122*, 6109-6117; (c) A. Gładysiak, T. N. Nguyen, J. A. R. Navarro, M. J. Rosseinsky, K. C. Stylianou, *Chem. Eur. J.* **2017**, *23*, 13602-13606.

[14] J. H. Lee, R. L. Siegelman, L. Maserati, T. Rangel, B. A. Helms, J. R. Long, J. B. Neaton, *Chem. Sci.* **2018**, *9*, 5197-5206.

[15] G. Brunet, D. A. Safin, M. Z. Aghaji, K. Robeyns, I. Korobkov, T. K. Woo, M. Murugesu, *Chem. Sci.* **2017**, *8*, 3171-3177.

[16] Y.-Q. Hu, M.-Q. Li, Y. Wang, T. Zhang, P.-Q. Liao, Z. Zheng, X.-M. Chen, Y.-Z. Zheng, *Chem. Eur. J.* **2017**, *23*, 8409-8413.

[17] H. A. Benesi, J. H. Hildebrand, *J. Am. Chem. Soc.* **1949**, *71*, 2703-2707.

[18] (a) M.-H. Zeng, Q.-X. Wang, Y.-X. Tan, S. Hu, H.-X. Zhao, L.-S. Long, M. Kurmoo, *J. Am. Chem. Soc.* **2010**, *132*, 2561-2563; (b) S. Horike, M. Sugimoto, K. Kongpatpanich, Y. Hijikata, M. Inukai, D. Umeyama, S. Kitao, M. Seto, S. Kitagawa, *J. Mater. Chem. A* **2013**, *1*, 3675-3679; (c) D. Y. Lee, E. K. Kim, N. K. Shrestha, D. W. Boukhvalov, J. K. Lee, S. H. Han, *ACS Appl. Mater. Interfaces* **2015**, *7*, 18501-18507.

[19] L. Sun, S. S. Park, D. Sheberla, M. Dincă, *J. Am. Chem. Soc.* **2016**, *138*, 14772-14782.

[20] (a) S. Goswami, D. Ray, K.-i. Otake, C.-W. Kung, S. J. Garibay, T. Islamoglu, A. Atilgan, Y. Cui, C. J. Cramer, O. K. Farha, J. T. Hupp, *Chem. Sci.* **2018**, *9*, 4477-4482; (b) C. Schneider, D. Ukaj, R. Koerver, A. A. Talin, G. Kieslich, S. P. Pujari, H. Zuilhof, J. Janek, M. D. Allendorf, R. A. Fischer, *Chem. Sci.* **2018**.

[21] J. P. Perdew, M. Levy, *Phys. Rev. Lett.* **1983**, *51*, 1884-1887.

[22] J. L. Lyons, C. G. Van de Walle, *npj Comput. Mater.* **2017**, *3*, 12.

[23] K. C. Stylianou, R. Heck, S. Y. Chong, J. Bacsa, J. T. A. Jones, Y. Z. Khimyak, D. Bradshaw, M. J. Rosseinsky, *J. Am. Chem. Soc.* **2010**, *132*, 4119-4130.

[24] V. Dyadkin, P. Pattison, V. Dmitriev, D. Chernyshov, *J. Synchrotron Rad.* **2016**, *23*, 825-829.

[25] RigakuOxfordDiffraction, 1.171.38.43 ed., **2015**.

[26] G. Sheldrick, *Acta Cryst. Sect. A* **2015**, *71*, 3-8.

[27] G. Sheldrick, *Acta Cryst. Sect. C* **2015**, *71*, 3-8.

[28] O. V. Dolomanov, L. J. Bourhis, R. J. Gildea, J. A. K. Howard, H. Puschmann, *J. Appl. Cryst.* **2009**, *42*, 339-341.

[29] C. F. Macrae, I. J. Bruno, J. A. Chisholm, P. R. Edgington, P. McCabe, E. Pidcock, L. Rodriguez-Monge, R. Taylor, J. van de Streek, P. A. Wood, *J. Appl. Cryst.* **2008**, *41*, 466-470.

[30] A. L. Spek, 120716 ed., **2016**.

[31] J. Rodríguez-Carvajal, *Physica B* **1993**, *192*, 55-69.

[32] J. P. Perdew, A. Ruzsinszky, G. I. Csonka, O. A. Vydrov, G. E. Scuseria, L. A. Constantin, X. Zhou, K. Burke, *Phys. Rev. Lett.* **2008**, *100*, 136406.

[33] (a) P. Giannozzi, S. Baroni, N. Bonini, M. Calandra, R. Car, C. Cavazzoni, D. Ceresoli, G. L. Chiarotti, M. Cococcioni, I. Dabo, A. Dal Corso, S. de Gironcoli, S. Fabris, G. Fratesi, R. Gebauer, U. Gerstmann, C. Gougoussis, A. Kokalj, M. Lazzeri, L. Martin-Samos, N. Marzari, F. Mauri, R. Mazzarello, S. Paolini, A. Pasquarello, L. Paulatto, C. Sbraccia, S. Scandolo, G. Sclauzero, A. P. Seitsonen, A. Smogunov, P. Umari, R. M. Wentzcovitch, *J. Phys. Condens. Matter* **2009**, *21*, 395502; (b) P. Giannozzi, O. Andreussi, T. Brumme, O. Bunau, M. B. Nardelli, M. Calandra, R. Car, C. Cavazzoni, D. Ceresoli, M. Cococcioni, N. Colonna, I. Carnimeo, A. D. Corso, S. d. Gironcoli, P. Delugas, J. R. A. DiStasio, A. Ferretti, A. Floris, G. Fratesi, G. Fugallo, R. Gebauer, U. Gerstmann, F. Giustino, T. Gorni, J. Jia, M. Kawamura, H. Y. Ko, A. Kokalj, E. Küçükbenli, M. Lazzeri, M. Marsili, N. Marzari, F. Mauri, N. L. Nguyen, H. V. Nguyen, A. Otero-de-la-Roza, L. Paulatto, S. Poncé, D. Rocca, R. Sabatini, B. Santra, M. Schlipf, A. P. Seitsonen, A. Smogunov, I. Timrov, T. Thonhauser, P. Umari, N. Vast, X. Wu, S. Baroni, *J. Phys. Condens. Matter* **2017**, *29*, 465901.

[34] (a) T. Thonhauser, V. R. Cooper, S. Li, A. Puzder, P. Hyldgaard, D. C. Langreth, *Phys. Rev. B* **2007**, *76*, 125112; (b) D. C. Langreth, B. I. Lundqvist, S. D. Chakarova-Käck, V. R. Cooper, M. Dion, P. Hyldgaard, A. Kelkkanen, J. Kleis, K. Lingzhu, L. Shen, P. G. Moses, E. Murray, A. Puzder, H. Rydberg, E. Schröder, T. Thonhauser, *J. Phys. Condens. Matter* **2009**, *21*, 084203; (c) K. Berland, V. R. Cooper, K. Lee, E. Schröder, T. Thonhauser, P. Hyldgaard, B. I. Lundqvist, *Reports Prog. Phys.* **2015**, *78*, 066501.

[35] C. Elsässer, M. Fähnle, C. T. Chan, K. M. Ho, *Phys. Rev. B* **1994**, *49*, 13975-13978.

Entry for the Table of Contents

COMMUNICATION

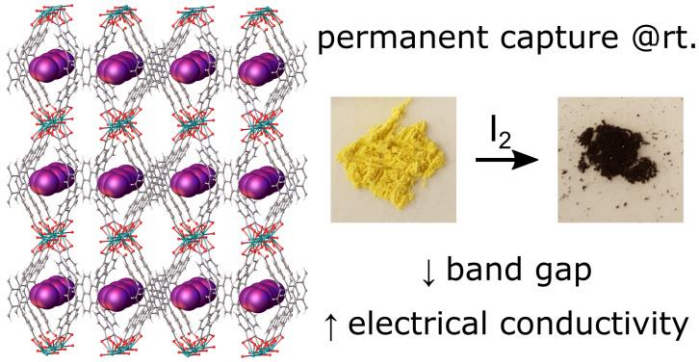

Trapped forever. A pyrene-based MOF, **SION-8**, efficiently adsorbs vapour iodine, however, unlike in other known materials, this capture is permanent at room temperature. The formation of the stable charge transfer complex **SION-8⊃I_2** can be tracked with conspicuous colour and electrical conductivity changes.

Andrzej Gładysiak,†[a] Tu N. Nguyen,†[a] Mariana Spodaryk,[b] Jung-Hoon Lee,[c,d] Jeffrey B. Neaton,[c,d,e] Andreas Züttel,[b] and Kyriakos C. Stylianou[a]*

Page No. – Page No.

Incarceration of iodine in a pyrene-based metal–organic framework